

Intelligent Signal Processing for BackScatter Radio Communications & Networking

Assoc. Prof. Aggelos Bletsas
School of ECE, TU Crete

Joint work with my students/colleagues at TU Crete.
Special thanks to P.N. Alevizos and G. Vougioukas



Nov. 8 2017

Agenda

- 1 BackScatter Radio: Tags/Reflectors
 - Intro
 - Fundamentals
- 2 BackScatter Radio: Derived Detectors
 - Symbol-by-Symbol
 - Sequence Detection
 - Notes on RFID/Gen2 and Embedded Receivers
- 3 BackScatter Radio: Networks/Apps
 - MultiStatic Networks for Extended Coverage
 - Networks/Apps

What? Where?

What/Where:

- **What:** " Ultra low-power communication by means of reflection - No amplifiers, mixers, filters or power-consuming *signal conditioning/processing* at the tag/reflector".
- **Where:** spy industry, RFIDs, medical implants, coming (really) low-power IoT!

Questions for today:

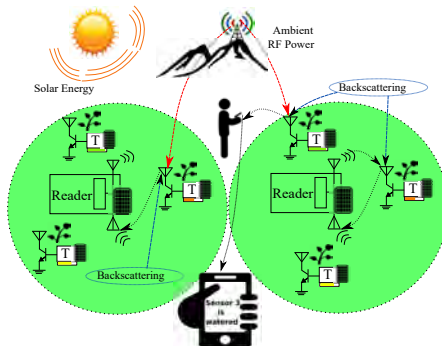
- Maximum range/coverage?
- Connection to satellite/underwater communications?
- "Can you measure the water soil moisture of your favorite flower using your cellphone" ?

Why?



- 1945 Theremin's "The Thing" or "Great Seal Bug" (wikipedia photos)...

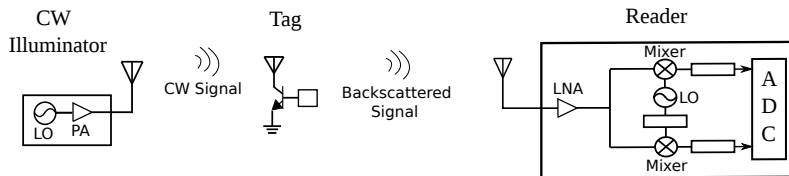
Why? Our vision...[1]



- 80-85% of total water is consumed for agriculture purposes.
- Intelligent plant irrigation: Save $\approx 30\%$ of water!

[1] P. Alevizos, "Intelligent scatter radio, RF harvesting analysis, and resource allocation for ultra-low-power Internet-of-Things," Ph.D. dissertation, School of ECE, Technical University of Crete, Chania, Greece, 2017, advisor: A. Bletsas.

Principle: Tag Reflection

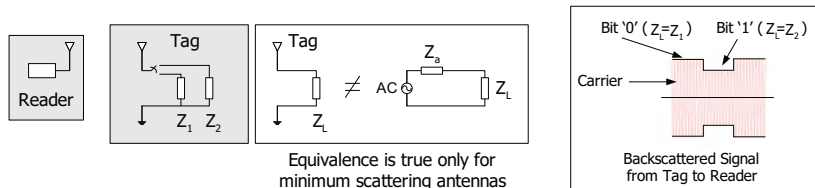


- Monostatic Architecture (RFID): illuminator + reader = same unit (common local oscillator - LO) [2], multi-antenna monostatic [3].
- Bistatic Architecture (WSNs/ambient): illuminator \neq reader (distinct units).

[2] G. Vannucci, A. Bletsas, and D. Leigh, "A software-defined radio system for backscatter sensor networks", IEEE Trans. Wireless Commun., vol. 7, no. 6, pp. 2170-2179, Jun. 2008. Conf. version at IEEE PIMRC 2007, Athens, Greece.

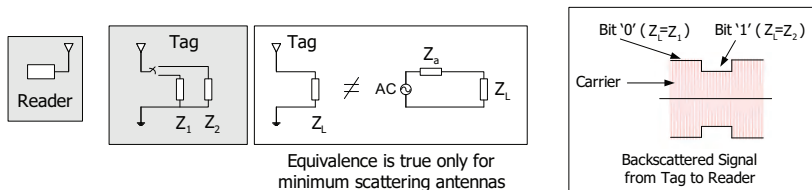
[3] J.D. Griffin and G.D. Durgin, "Gains for RF tags using multiple antennas", IEEE Trans. Antennas Propag., vol. 56, no. 2, pp. 563-570, Feb. 2008.

Simplest case: Tag Reflection with 2 Loads



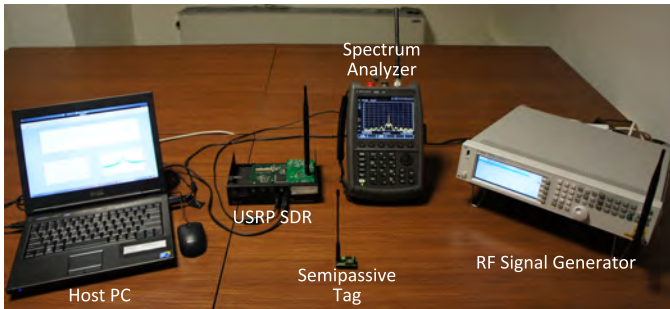
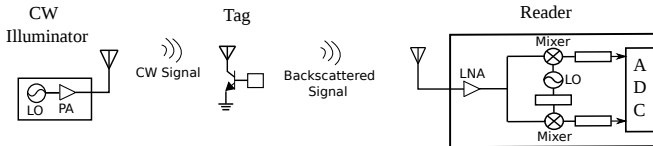
- Modified Reflection Coefficient: $\Gamma_1 = \frac{Z_2 - Z_a^*}{Z_2 + Z_a^*}$, $\Gamma_0 = \frac{Z_1 - Z_a^*}{Z_1 + Z_a^*}$,
 Z_a (complex) tag antenna characteristic impedance.
- Backscattered Tag Signal Baseband Equivalent: $A_s - \Gamma_i$,
 A_s (complex) load-independent tag antenna structural mode.

Tag Reflection with 2 Loads: OOK vs FSK

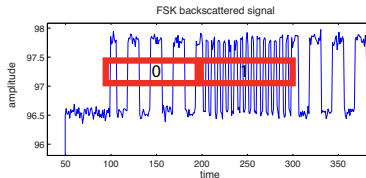
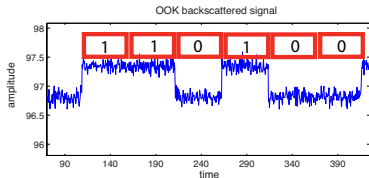


- OOK: terminate at load for whole bit duration T , i.e., Z_1 (Γ_0) for bit '0', Z_2 (Γ_1) for bit '1'.
- FSK: alternatively switch between two loads for bit duration, with switching frequency F_0 for bit '0' or F_1 for bit '1'. Utilize a 50% duty-cycle switching signal (with period $1/F_i$).

Tests with custom tags and SDR

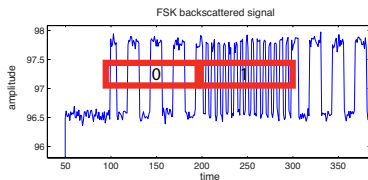
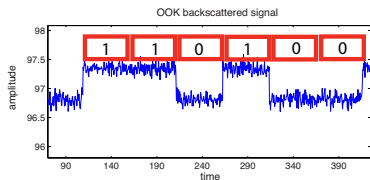


Tag Reflection with 2 Loads: OOK vs FSK



- OOK: terminate at load for whole bit duration T , i.e., Z_1 (Γ_0) for bit '0', Z_2 (Γ_1) for bit '1'.
- FSK: alternatively switch between two loads for bit duration, with switching frequency F_0 for bit '0' or F_1 for bit '1'. Utilize a 50% duty-cycle pulse-train switching signal (with period $1/F_i$).

Tag Reflection with 2 Loads: OOK Tag Equations [4-7]



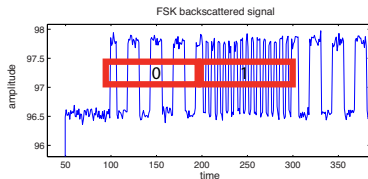
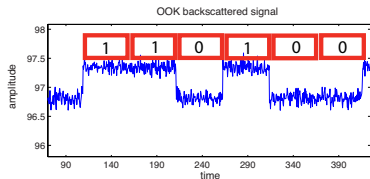
$$\text{Tag Bit } n \Rightarrow \Gamma_{\text{tag}} = \Gamma_0 \text{ for } x_n = -1, \Gamma_{\text{tag}} = \Gamma_1 \text{ for } x_n = +1 : \quad (1)$$

$$A_s - \Gamma_{\text{tag}} = \left(A_s - \frac{\Gamma_0 + \Gamma_1}{2} \right) + x_n \frac{\Gamma_0 - \Gamma_1}{2}, \quad x_n \in \pm 1 \quad (2)$$

$$x_{\text{Tag}}(t) = \left(A_s - \frac{\Gamma_0 + \Gamma_1}{2} \right) + \frac{\Gamma_0 - \Gamma_1}{2} x_n \Pi_T(t - nT), \quad t \in [nT, (n+1)T), \quad (3)$$

$\Pi_T(t) = 1$ for $t \in [0, T)$ and zero elsewhere.

Tag Reflection with 2 Loads: FSK Tag Equations [4-7]

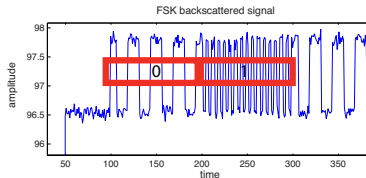
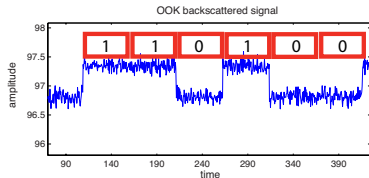


$$\text{Tag Bit } n \Rightarrow F_{\text{tag}}^{\text{sw}} \triangleq F_{x_n=-1} = F_0, F_{\text{tag}}^{\text{sw}} \triangleq F_{x_n=+1} = F_1, F_{x_n} \in \{F_0, F_1\} \quad (4)$$

$$x_{\text{Tag}}(t) = \left(A_s - \frac{\Gamma_0 + \Gamma_1}{2} \right) + \frac{\Gamma_0 - \Gamma_1}{2} b_{F_{x_n}}(t - nT), t \in [nT, (n+1)T), \quad (5)$$

$b_F(t)$: (periodic) pulse train with fundamental frequency $F \in \{F_0, F_1\}$ and duration equal to bit duration T ($T \gg \max(1/F_0, 1/F_1)$).

Tag Reflection with 2 Loads: FSK Tag Equations [4–7]



$$\text{Tag Bit } n \Rightarrow F_{\text{tag}}^{\text{sw}} \triangleq F_{x_n} \equiv F_n \in \{F_0, F_1\} \quad (6)$$

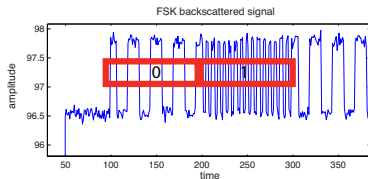
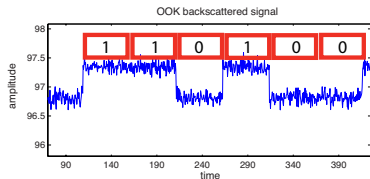
$$x_{\text{Tag}}(t) = \left(A_s - \frac{\Gamma_0 + \Gamma_1}{2} \right) + \frac{\Gamma_0 - \Gamma_1}{2} b_{F_n}(t - nT), \quad t \in [nT, (n+1)T).$$

For $b_F(t)$ 50% duty-cycle, pulse train, even $b_{F_n}(t) = b_{F_n}(-t)$:

$$b_{F_n}(t) = \frac{4}{\pi} \sum_{k=0}^{+\infty} \frac{1}{2k+1} \cos[2\pi(2k+1)F_n t]. \quad (7)$$

- Only odd-order harmonics. For odd $b_F(t)$ instead, only sine terms...

Tag Reflection with 2 Loads: FSK Tag Equations [4–7]



$$\text{Tag Bit } n \Rightarrow F_{\text{tag}}^{\text{sw}} \triangleq F_{x_n} \equiv F_n \in \{F_0, F_1\} \quad (8)$$

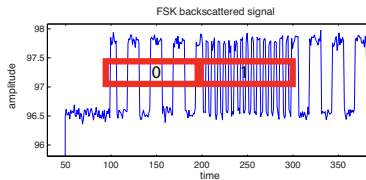
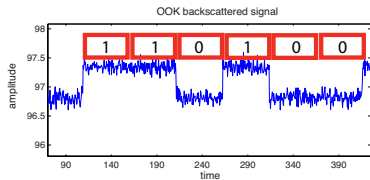
$$x_{\text{Tag}}(t) = \left(A_s - \frac{\Gamma_0 + \Gamma_1}{2} \right) + \frac{\Gamma_0 - \Gamma_1}{2} b_{F_n}(t - nT), \quad t \in [nT, (n+1)T).$$

For $b_F(t)$ 50% duty-cycle, pulse train, **odd** $b_{F_n}(-t) = -b_{F_n}(t)$:

$$b_{F_n}(t) = \frac{4}{\pi} \sum_{k=0}^{+\infty} \frac{1}{2k+1} \sin [2\pi(2k+1)F_n t]. \quad (9)$$

- In practice, there is remaining phase Φ during tag modulation...

Tag Reflection with 2 Loads: FSK Tag Equations [4–7]



$$\text{Tag Bit } n \Rightarrow F_{\text{tag}}^{\text{sw}} \triangleq F_{x_n} \equiv F_n \in \{F_0, F_1\} \quad (10)$$

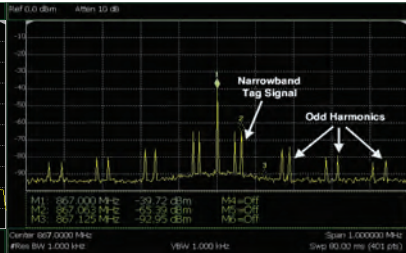
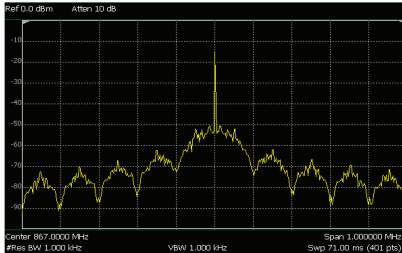
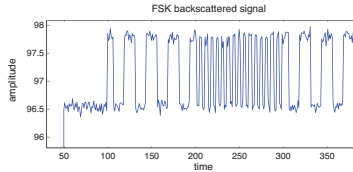
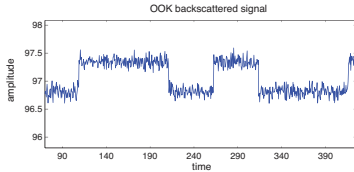
$$x_{\text{Tag}}(t) = \left(A_s - \frac{\Gamma_0 + \Gamma_1}{2} \right) + \frac{\Gamma_0 - \Gamma_1}{2} b_{F_n}(t - nT), \quad t \in [nT, (n+1)T).$$

For $b_F(t)$ 50% duty-cycle, pulse train, **even** $b_{F_n}(t) = b_{F_n}(-t)$:

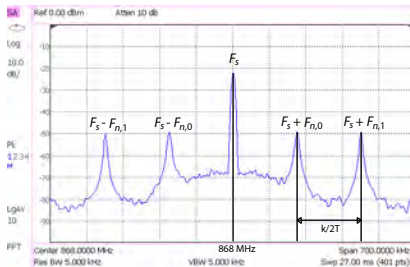
$$b_{F_n}(t) = \frac{4}{\pi} \sum_{k=0}^{+\infty} \frac{1}{2k+1} \cos[2\pi(2k+1)F_n t + \Phi]. \quad (11)$$

- Tag (remaining) phase Φ , due to imperfect tag modulation, matters!
- Simplify notation: $b_{F_n}(t) \equiv b_n(t)$, $n \in \{0, 1\}$.

Tag Reflection with 2 Loads: OOK vs FSK



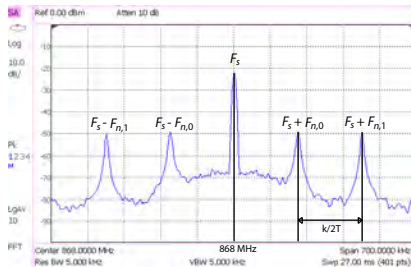
Tag Reflection with 2 Loads: OOK or FSK?



$$\{F_{\nu,0}, F_{\nu,1}\}, \nu = 1, 2, \dots, N \text{ Tags...}$$

- OOK: RFID industry (GEN2) (+), clutter around carrier freq. (-), need for receiver at Tag for CSMA (framed Aloha) (-)...

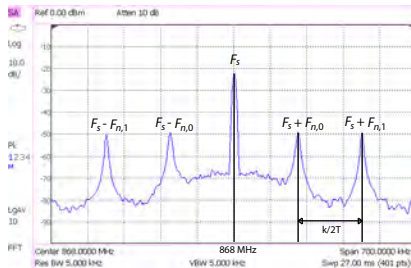
Tag Reflection with 2 Loads: OOK or FSK?



$$\{F_{\nu,0}, F_{\nu,1}\}, \nu = 1, 2, \dots, N \text{ Tags...}$$

- FSK: power-limited regime (+), easy, Tag receiver-less networking (FDMA with common carrier freq.) (+), ideal for low bitrate (bandwidth) sensors (+), non-ideal for high bitrate sensors (-)...

Tag Reflection with 2 Loads: OOK or FSK?



$$\{F_{\nu,0}, F_{\nu,1}\}, \nu = 1, 2, \dots, N \text{ Tags...}$$

- FSK: what about odd harmonics? Don't you need pulse shaping with multiple loads?

Tag Reflection and Pulse Shaping: 2 vs multiple Loads

- **Answer: NO!**

Lemma

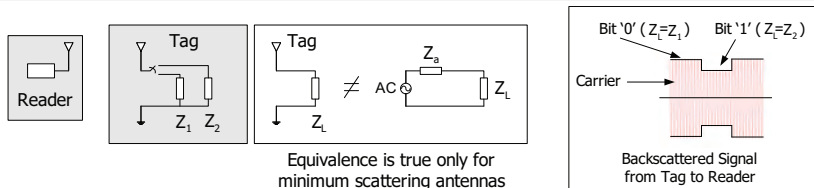
Pulse shaping in FSK with only two loads is possible - see MSK work with backscatter radio, circa 2007 – 2008 [2]!

- Minimum Shift Keying (MSK): FSK without discontinuities at bit boundaries, PSD drops with fourth power of frequency - see PLL implementation in the paper above.
- Pulse shaping in FSK with multiple loads: rotating phasor that shifts tag signal spectrum at left or right of the illuminating carrier frequency [8].

[2] G. Vannucci, A. Bletsas, and D. Leigh, "A software-defined radio system for backscatter sensor networks", IEEE Trans. Wireless Commun., vol. 7, no. 6, pp. 2170-2179, Jun. 2008. Conf. version at IEEE PIMRC 2007, Athens, Greece.

[8] V. Iyer, V. Talla, B. Kellogg, S. Gollakota, and J. Smith, "Inter-technology backscatter: Towards internet connectivity for implanted devices", in Proceedings of the 2016 ACM SIGCOMM, Florianopolis, Brazil.

Tag Reflection with 2 Loads: things to remember...



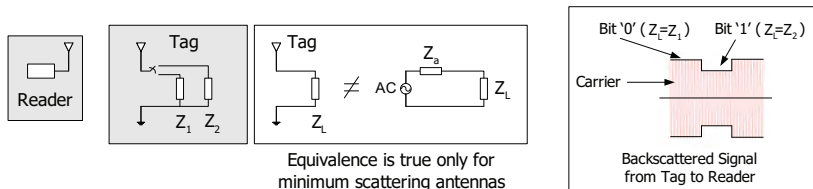
Current mindset for backscattering:

- for minimum scattering antennas only $|\Gamma_0 - \Gamma_1|$ matters!
- for *coherent* (i.e., minimum distance) detection, $|(A_s - \Gamma_0) - (A_s - \Gamma_1)| = |\Gamma_1 - \Gamma_0|$ matters!

However,

- For non-minimum scattering antennas [9] or certain house keeping tasks *before* detection, A_s matters... controls the carrier...
- ...think of bistatic setups, where emitter-to-reader link is blocked... CFO estimation?

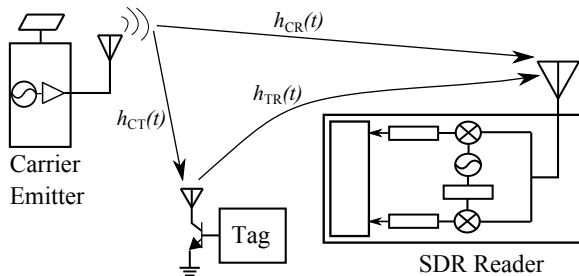
Tag Reflection with 2 Loads: things to remember...



- Measurement method for A_s estimation can be found in [9].

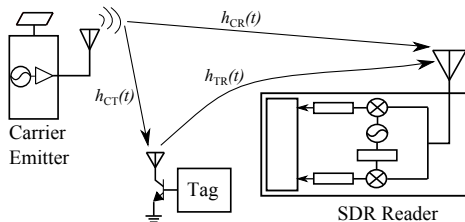
[9] A. Bletsas, A. G. Dimitriou, and J. Sahalos, "Improving backscatter radio tag efficiency", IEEE Trans. Microw. Theory Techn., vol. 58, no. 6, pp. 1502 - 1509, Jun. 2010.

Wireless Model



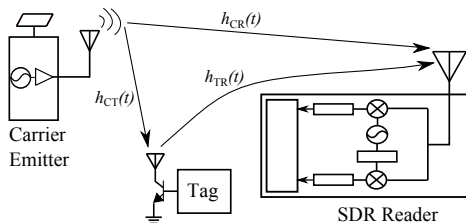
- Flat fading: $h_m(t) = h_m$, $m \in \{CR, CT, TR\}$.
- $h_m(t) = a_m \delta(t - \tau_m)$, modeling channel amplitude and phase...
- This work can model asymmetric scenarios (as in *ambient*)...

Wireless Fading Models Assumed



- Flat Rician fading: $h_m(t) = h_m \sim \mathcal{CN}\left(\sqrt{\frac{\kappa_m}{\kappa_m+1}}\sigma_m, \frac{\sigma_m^2}{\kappa_m+1}\right)$, $m \in \{CR, CT, TR\}$.
- Similarly, flat Nakagami fading will be also assumed...
- This work can model asymmetric scenarios (as in *ambient*)...

Wireless Model

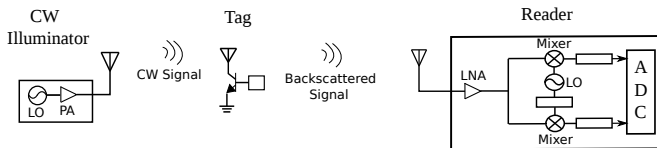


- Carrier emitter: $c(t) = \sqrt{2P_C} e^{-j(2\pi\Delta Ft + \Delta\phi)}$, modeling CFO ($\Delta F = 0$ for monostatic).
- Tag backscatters:

$$x_{\text{Tag}}^i(t) = \left((A_s - \frac{\Gamma_0 + \Gamma_1}{2}) + \frac{\Gamma_0 - \Gamma_1}{2} b_i(t) \right) s a_{\text{CT}} e^{-j\phi_{\text{CT}}} c(t), \quad i \in \mathbb{B}.$$
- Reader receives:

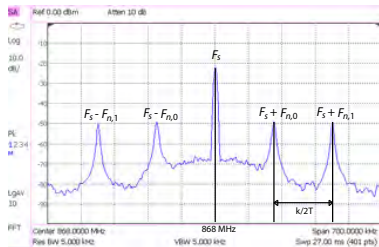
$$y(t) = a_{\text{CR}} e^{-j\phi_{\text{CR}}} c(t) + a_{\text{TR}} e^{-j\phi_{\text{TR}}} x_{\text{Tag}}^i(t) + n(t).$$

RFID/Backscatter Radio Inherent Problems



- Inherent problems:
 - Large path-loss attenuation \implies Limited range.
 - Passive tags \implies Powering issues \implies Limited range.
 - High bitrate \implies Reduced energy per bit \implies Limited range.
- This work:
 - Short-packet communication.
 - Optimal receiver design for scatter radio signals.

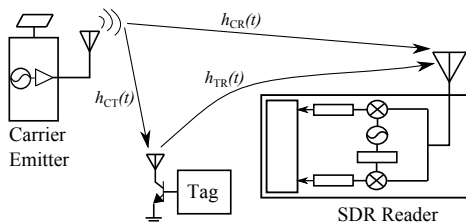
2-load Tag Reflection Principles Reminder!



$$\{F_{\nu,0}, F_{\nu,1}\}, \nu = 1, 2, \dots, N \text{ Tags...} \quad (12)$$

- Switching between two loads with rate $F_i, i \in \{0, 1\}$ results to $F_c \pm F_i$...
- 4 instead of 2 peaks \Rightarrow 4 matched filters!
- Coherent detection: $|F_0 - F_1| = k/(2T)$,
 Noncoherent detection: $|F_0 - F_1| = k/T, k \in \mathcal{Z}$.

Noncoherent Bistatic FSK Symbol-by-Symbol Detector



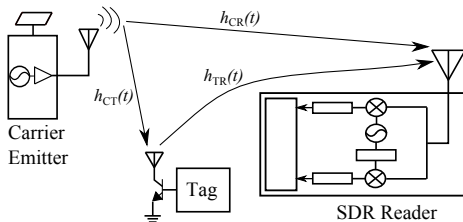
- Decouple Emitter (illuminator) from Reader, work with (simpler) FSK [4–7].
- Caveat: no phase continuity/PSD compared to MSK [2]...

[4] J. Kimionis, A. Bletsas, and J. N. Sahalos, "Design and implementation of RFID systems with software-defined radio", in Proc. IEEE European Conf. on Antennas and Propagation (EuCAP), Prague, Czech Republic, Mar. 2012, pp. 3464-3468.

[5] —, "Bistatic backscatter radio for tag read-range extension", in Proc. IEEE RFID Techn. and Applications (RFID-TA), Nice, France, Nov. 2012.

[7] —, "Increased range bistatic scatter radio", IEEE Trans. Commun., vol. 62, no. 3, pp. 1091-1104, Mar. 2014.

Noncoherent Bistatic FSK Symbol-by-Symbol Detector



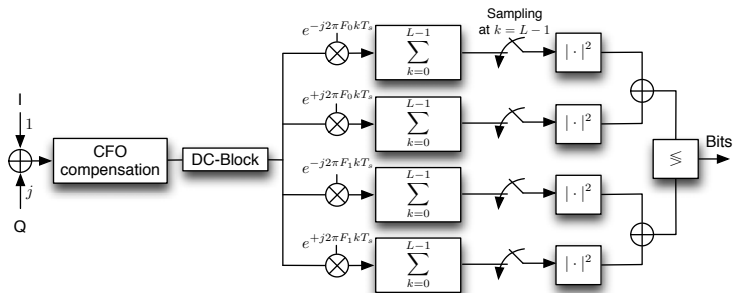
- Decouple Emitter (illuminator) from Reader, work with (simpler) FSK [4–7].
- *Ambient backscatter* (SIGCOMM Aug. 2013 [10]) is a bistatic architecture!

[4] J. Kimionis, A. Bletsas, and J. N. Sahalos, "Design and implementation of RFID systems with software-defined radio", in Proc. IEEE European Conf. on Antennas and Propagation (EuCAP), Prague, Czech Republic, Mar. 2012, pp. 3464-3468.

[5] —, "Bistatic backscatter radio for tag read-range extension", in Proc. IEEE RFID Techn. and Applications (RFID-TA), Nice, France, Nov. 2012.

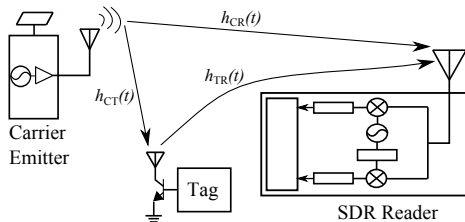
[7] —, "Increased range bistatic scatter radio", IEEE Trans. Commun., vol. 62, no. 3, pp. 1091-1104, Mar. 2014.

Noncoherent Symbol-by-Symbol Bistatic FSK [4–7]



- Housekeeping: periodogram-based CFO compensation, DC block...
- Detection: $|r_0^+|^2 + |r_0^-|^2$ vs $|r_1^+|^2 + |r_1^-|^2$
- Why not $|r_0^+| + |r_0^-|$ vs $|r_1^+| + |r_1^-|$???

Coherent Symbol-by-Symbol/Sequence Bistatic FSK



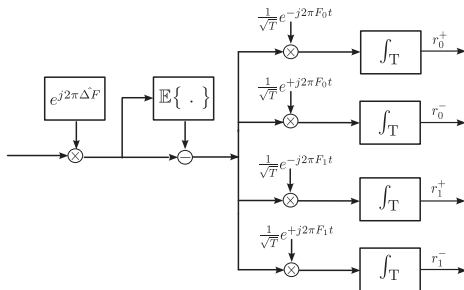
Important Simplification in [11]:

- Baseband signal for scatter radio FSK modulation [Theorem 1, [11]]:

$$\mathbf{r} = [r_0^+ \ r_0^- \ r_1^+ \ r_1^-]^T = h\sqrt{\frac{E}{2}}[e^{+j\Phi_0} \ e^{-j\Phi_0} \ e^{+j\Phi_1} \ e^{-j\Phi_1}]^T \odot \mathbf{s}_i + \mathbf{n}. \quad (13)$$

[11] N. Fasarakis-Hilliard, P. N. Alevizos, and A. Bletsas, "Coherent detection and channel coding for bistatic scatter radio sensor networking," *IEEE Trans. Commun.*, vol. 63, pp. 1798–1810, May 2015.

Coherent Symbol-by-Symbol/Sequence Bistatic FSK [11]



$$\mathbf{r} = [r_0^+ \ r_0^- \ r_1^+ \ r_1^-]^T = h\sqrt{\frac{E}{2}}[e^{+j\phi_0} \ e^{-j\phi_0} \ e^{+j\phi_1} \ e^{-j\phi_1}]^T \odot \mathbf{s}_i + \mathbf{n}, \quad (14)$$

$$\mathbf{E} = \kappa^2 P_C |\Gamma_0 - \Gamma_1|^2 \mathbf{s}^2 T, \quad h = a_{CT} a_{TR} e^{(\phi_{CT} + \phi_{TR} + \Delta\phi + \angle(\Gamma_0 - \Gamma_1))}, \quad (15)$$

$$\mathbf{s}_i = [1 - i \ 1 - i \ i \ i]^T, \quad i \in \{0, 1\}, \quad \mathbf{n} \sim \mathcal{CN}\left(\mathbf{0}_4, \frac{N_0}{2} \mathbf{I}_4\right). \quad (16)$$

Coherent Symbol-by-Symbol/Sequence Bistatic FSK [11]

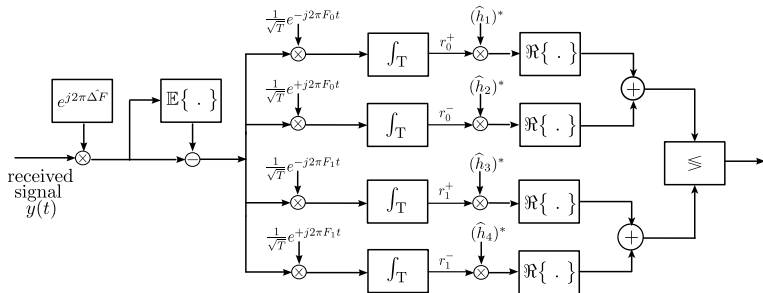
$$\mathbf{r} = [r_0^+ \ r_0^- \ r_1^+ \ r_1^-]^\top = h \sqrt{\frac{E}{2}} [e^{+j\Phi_0} \ e^{-j\Phi_0} \ e^{+j\Phi_1} \ e^{-j\Phi_1}]^\top \odot \mathbf{s}_i + \mathbf{n}, \quad (17)$$

- Estimate with preamble/LS $\hat{\mathbf{h}} = [\hat{h}_1 \ \hat{h}_2 \ \hat{h}_3 \ \hat{h}_4]^\top$ of $\mathbf{h} = h \sqrt{\frac{E}{2}} [e^{+j\Phi_0} \ e^{-j\Phi_0} \ e^{+j\Phi_1} \ e^{-j\Phi_1}]^\top$.
- Perform ML:

$$b_i^{\text{ML}} = \arg \max_{b_i \in \{0,1\}} \exp \left\{ -\frac{2}{N_0} \|\mathbf{r} - \hat{\mathbf{h}} \odot \mathbf{s}_{b_i}\|^2 \right\} \quad (18)$$

$$\Leftrightarrow \mathcal{R} \left((\hat{h}_1)^* r_0^+ + (\hat{h}_2)^* r_0^- \right) \stackrel{\text{bit } 0}{\geq} \mathcal{R} \left((\hat{h}_3)^* r_1^+ + (\hat{h}_4)^* r_1^- \right) \quad (19)$$

Coherent Symbol-by-Symbol/Sequence Bistatic FSK [11]



- ML Symbol-by-Symbol detector (above)...
- ML Sequence detector also tested with Reed-Muller (RM) and BCH channel coded sequences!

Noncoherent Symbol-by-Symbol Bistatic FSK: HCHT

Work in [12], [13]:

- Statistics: $f(\mathbf{r}|i, h, \Phi) \equiv \mathcal{CN}(h \mathbf{x}_i(\Phi), N_0 \mathbf{I}_4)$, with
 $\mathbf{x}_i(\Phi) = \sqrt{\frac{E}{2}} [e^{+j\Phi_0}, e^{-j\Phi_0}, e^{+j\Phi_1}, e^{-j\Phi_1}]^T \odot \mathbf{s}_i, i \in \mathbb{B}$.

Lemma

Noncoherent Hybrid Composite Hypothesis-Testing (HCHT)
 Symbol-By-Symbol FSK Detection:

$$\arg \max_{i \in \mathbb{B}} \left\{ \mathbb{E}_{\Phi} \left[\max_{h \in \mathcal{C}} \ln[f(\mathbf{r}|i, h, \Phi)] \right] \right\} \iff |r_0^+|^2 + |r_0^-|^2 \stackrel{i=0}{\gtrsim} |r_1^+|^2 + |r_1^-|^2. \quad (20)$$

[12] P. N. Alevizos and A. Bletsas, "Noncoherent composite hypothesis testing receivers for extended range bistatic scatter radio WSNs," in *Proc. IEEE Int. Conf. on Commun.*, London, U.K., Jun. 2015.

[13] P. N. Alevizos, A. Bletsas, and G. N. Karystinos, "Noncoherent short packet detection and decoding for scatter radio sensor networking," *IEEE Trans. Commun.*, vol. 65, no. 5, pp. 2128-2140, May 2017.

Noncoherent Symbol-by-Symbol Bistatic FSK: GLRT

Work in [12], [13]:

- Statistics: $f(\mathbf{r}|i, h, \Phi) \equiv \mathcal{CN}(h \mathbf{x}_i(\Phi), N_0 \mathbf{I}_4)$, with
 $\mathbf{x}_i(\Phi) = \sqrt{\frac{E}{2}} [e^{+j\Phi_0}, e^{-j\Phi_0}, e^{+j\Phi_1}, e^{-j\Phi_1}]^T \odot \mathbf{s}_i, i \in \mathbb{B}$.

Theorem

Noncoherent Generalized Likelihood-Ratio Test (GLRT)
 Symbol-By-Symbol FSK Detection:

$$\arg \max_{i \in \mathbb{B}} \left\{ \max_{\Phi \in [0, 2\pi)^2} \max_{h \in \mathbb{C}} \ln[f(\mathbf{r}|i, h, \Phi)] \right\} \iff |r_0^+| + |r_0^-| \underset{i=1}{\overset{i=0}{\geq}} |r_1^+| + |r_1^-|. \quad (21)$$

[12] P. N. Alevizos and A. Bletsas, "Noncoherent composite hypothesis testing receivers for extended range bistatic scatter radio WSNs," in *Proc. IEEE Int. Conf. on Commun.*, London, U.K., Jun. 2015.

[13] P. N. Alevizos, A. Bletsas, and G. N. Karystinos, "Noncoherent short packet detection and decoding for scatter radio sensor networking," *IEEE Trans. Commun.*, vol. 65, no. 5, pp. 2128-2140, May 2017.

Noncoherent Uncoded Sequence Detector: GLRT

- Static environments: Coherence time \geq Packet duration.
- Transmitted sequence: $\mathbf{i} = [i_1 \ i_2 \ \dots \ i_{N_s}]^T \in \mathbb{B}^{N_s}$.
- Received sequence: $\mathbf{r}_{1:N_s}$ with statistics

$$f(\mathbf{r}_{1:N_s} | \mathbf{i}, h, \Phi) \equiv \mathcal{CN}(h \mathbf{x}_i(\Phi), N_0 \mathbf{I}_{4N_s}). \quad (22)$$

- GLRT sequence detector:

$$\mathbf{i}_{\text{GLRT}} = \arg \max_{\mathbf{i} \in \mathbb{B}^{N_s}} \max_{\Phi \in [0, 2\pi)^2} \max_{h \in \mathbb{C}} \ln[f(\mathbf{r}_{1:N_s} | \mathbf{i}, h, \Phi)]. \quad (23)$$

Theorem

There exists algorithm that finds \mathbf{i}_{GLRT} with complexity $\mathcal{O}(N_s \log N_s)$, based on [14], [15], instead of $\mathcal{O}(2^{N_s})$

[15] P. N. Alevizos, Y. Fountzoulas, G. N. Karystinos, and A. Bletsas, "Log-linear-complexity GLRT-optimal noncoherent sequence detection for orthogonal and RFID-oriented modulations," *IEEE Trans. Commun.*, vol. 64, no. 4, pp. 1600–1612, Apr. 2016. [Conf. version \[14\] received ICASSP 2015 Best Paper Award.](#)

Noncoherent Coded Sequence Detector: HCHT

- Diminish long-bursts of fading: *interleaving* of depth D .
- Baseband coded signal using interleaving [16], [12], [13]:

$$\mathbf{r}_{1:N_c} = \begin{bmatrix} \mathbf{r}_1 \\ \mathbf{r}_2 \\ \vdots \\ \mathbf{r}_{N_c} \end{bmatrix} = \begin{bmatrix} h_1 \mathbf{x}_{c_1}(\Phi) \\ h_2 \mathbf{x}_{c_2}(\Phi) \\ \vdots \\ h_{N_c} \mathbf{x}_{c_{N_c}}(\Phi) \end{bmatrix} + \begin{bmatrix} \mathbf{n}_1 \\ \mathbf{n}_2 \\ \vdots \\ \mathbf{n}_{N_c} \end{bmatrix}. \quad (24)$$

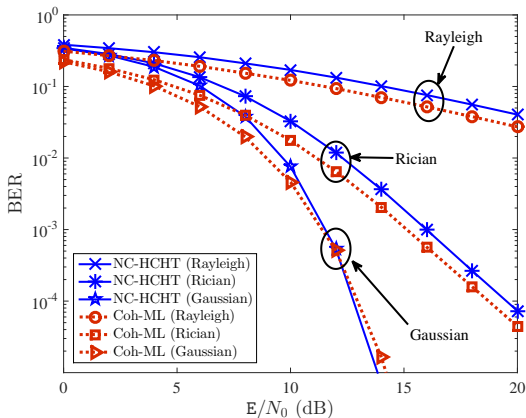
Theorem ([12], [13])

For $DT \geq T_{\text{coh}}$, noncoherent HCHT soft-decision decoding

$$\arg \max_{\mathbf{c} \in \mathcal{C}} \left\{ \mathbb{E}_{\Phi} \left[\max_{\mathbf{h} \in \mathcal{C}^{N_c}} \ln[f(\mathbf{r}_{1:N_c} | \mathbf{c}, \mathbf{h}, \Phi)] \right] \right\} \iff \arg \max_{\mathbf{c} \in \mathcal{C}} \sum_{n=1}^{N_c} w_n c_n, \quad (25)$$

where $w_n \triangleq |r_1^+(n)|^2 + |r_1^-(n)|^2 - (|r_0^+(n)|^2 + |r_0^-(n)|^2)$, $n = 1, 2, \dots, N_c$.

Numerical Results (1/2)



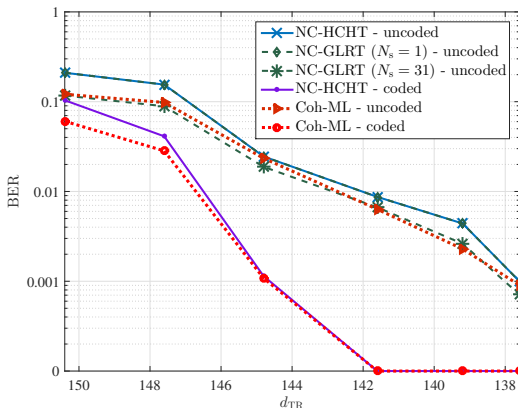
- Bit duration $T = 1$ msec, $T_{\text{coh}} = 100$ msec, 30 preamble (training) bits, 100-bit packet.

Experimental Results (1/2)



- $P_{TX} = 13$ dBm, receiver NF=7 – 12 dB, $d_{CT} = 8$ m, $T = 1$ msec, $F_1 = 2F_0 = 250$ kHz, 16 training (preamble) + 31 data coded bits.

Experimental Results (2/2)



- Housekeeping: Energy-based synchronization, Periodogram-based CFO estimation.

A note on RFID/Gen2

RFID industry Gen2 incorporates Miller and FM0 line coding. In FM0:

- level (line) always changes at bit boundaries...
- level (line) changes in the middle of bit, when bit is '0'...
- Gen2 exploits OOK not FSK...

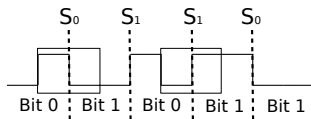


Figure: FM0 line coding.

- FM0 can be seen as orthogonal signaling...
- Technology on orthogonal signaling in the previous sections is readily applicable!

A note on RFID/Gen2

⇒ FM0 can be seen as orthogonal signaling! Observe half-bit before and half-bit after the bit of interest (totally $2T$ interval for bit duration T).

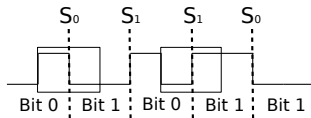
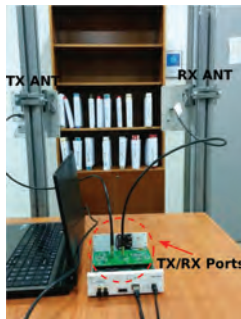


Figure: FM0 line coding.

- 2 possible T -duration orthogonal waveforms: S_0 and $S_1 \Rightarrow 2$ filters!
- $\mathbf{r} = [r_1 \ r_2]^T = h \sqrt{E} \mathbf{e}_i + \mathbf{n}$, $i \in \{0, 1\}$,
 $h \in \mathcal{C}$, $\mathbf{e}_0 = [1 \ 0]^T$, $\mathbf{e}_1 = [0 \ 1]^T$, $\mathbf{n} \sim \mathcal{CN}(\mathbf{0}, N_0 \mathbf{I}_2)$

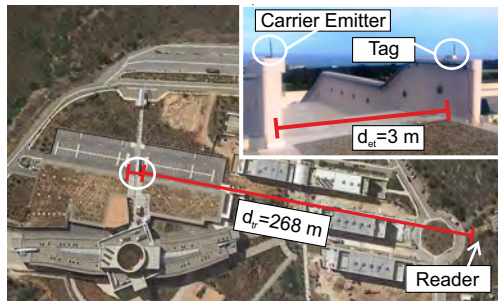
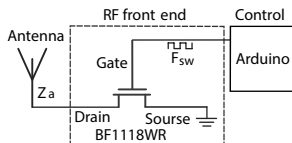
A note on RFID/Gen2



- Exploit Gen2 preambles, estimate channel and perform coherent detection with (differential) orthogonal signaling [17].
- Full SDR chain for Gen2/FM0 RFID, open source code [17]!

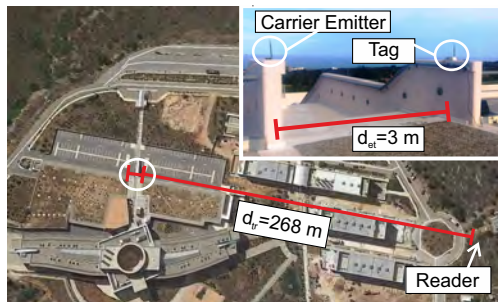
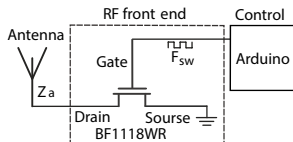
[17] N. Kargas, F. Mavromatis, and A. Bletsas, "Fully-coherent reader with commodity SDR for Gen2 FM0 and computational RFID," *IEEE Wireless Commun. Lett.*, vol. 4, no. 6, pp. 617–620, Dec. 2015.

A note on Embedded Receivers [18]



- Marconi Radio Embedded Receivers, Bistatic Architecture...
- Tag also backscatters preamble/protocol bits that embedded receiver expects...
- High sensitivity embedded receivers \Rightarrow extended ranges!

A note on Embedded Receivers [18]



- Bluetooth low energy (BLE) receiver backscatter reception [19].
- FSK, SI1064 or TI CC1101, Tx power +13 dBm [18].

[18] G. Vougioukas, S. N. Daskalakis, and A. Bletsas, "Could battery-less scatter radio tags achieve 270-meter range?", in Proc. IEEE Wireless Power Transfer Conf. (WPTC), Aveiro, Portugal, May 2016.

[19] J. F. Ensworth and M. S. Reynolds, "Every smart phone is a backscatter reader: Modulated backscatter compatibility with bluetooth 4.0 low energy (BLE) devices", in Proc. IEEE RFID, San Diego, CA, Apr. 2015.

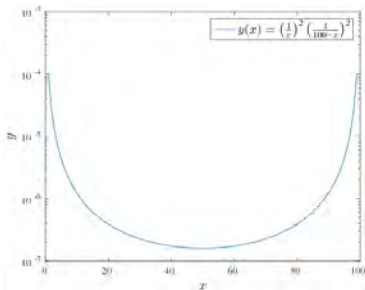
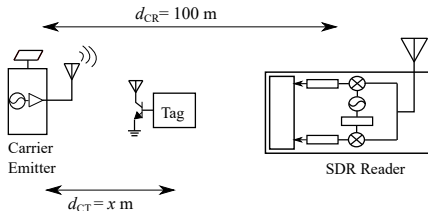
A note on Embedded Receivers [18]



- FSK, SI1064 or TI CC1101, Tx power +13 dBm [18].
- LORA backscatter reception [20]...
- ...with about 20 dB additional illuminator Tx power and about 30 dB higher sensitivity (due to smaller bandwidth), compared to [18].
- REMEMBER: 100 times smaller rate/bandwidth \Rightarrow 20 dB higher sensitivity...

[20] V. Talla, M. Hesar, B. Kellogg, A. Naja, J. R. Smith and S. Gollakota, "Lora backscatter: Enabling the vision of ubiquitous connectivity", Proc. ACM Interact. Mob. Wearable Ubiquitous Technol., vol. 1, no. 3, Sep. 2017.

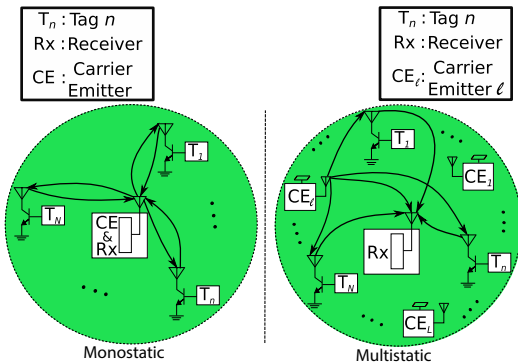
Bistatic (vs Monostatic) Helps!



- Asymmetric scatter radio architecture can reduce path-loss:
 - $PL \propto y(x) = \left(\frac{1}{x}\right)^2 \left(\frac{1}{100-x}\right)^2$.
 - $y(x)$ is minimized at $x = d/2 = 50\text{ m}$.
 - $y(x)$ increases as $x \rightarrow 0$ or $x \rightarrow 100$.

[1] P. Alevizos, "Intelligent scatter radio, RF harvesting analysis, and resource allocation for ultra-low-power Internet-of-things", Ph.D. dissertation, School of ECE, Technical University of Crete, Chania, Greece, 2017.

Why don't we exploit several emitters?



- Several emitters/illuminators: multistatic architecture.
- Does multistatic outperform state-of-the-art monostatic architecture?

BER & Diversity Order Analysis (1/2) [1] [21]

Theorem

Under dyadic Nakagami fading, the BER of monostatic architecture with ML coherent detection can be bounded as

$$\mathbb{P}\left(e_{l,n}^{[m]}\right) \leq \frac{1}{2} \left(\frac{M_n + M_n^2}{2 \text{SNR}_n^{[m]}} \right)^{\frac{M_n}{2}} U\left(\frac{M_n}{2}, \frac{1}{2}, \frac{M_n + M_n^2}{2 \text{SNR}_n^{[m]}}\right), \quad (26)$$

where M_n is the Nakagami parameter for link TR, and $U(\cdot, \cdot, \cdot)$ is given in [Eq. (13.4.4), 10], and $\text{SNR}_n^{[m]}$ is the average received SNR for monostatic system.

For dyadic Rayleigh fading ($M_n = 1$), the diversity order is $\frac{1}{2}$.

- The above BER bound coincides with noncoherent envelope monostatic scatter radio detection!

[10] F. W. J. Olver et. al, *NIST handbook of mathematical functions*, 2010.

BER Analysis & Diversity Order (2/2)[1] [21]

Theorem

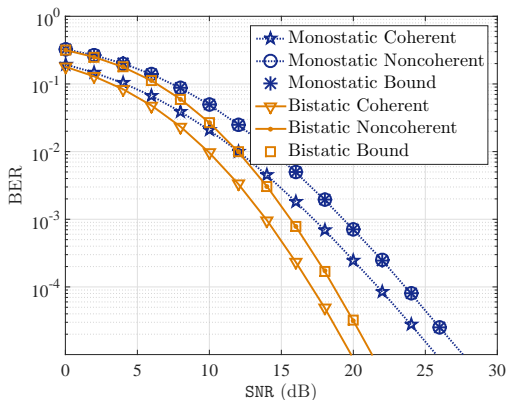
Under dyadic Nakagami fading, the BER of bistatic architecture with ML coherent detection can be bounded as

$$\mathbb{P}\left(e_{l,n}^{[b]}\right) \leq \frac{1}{2} \left(\frac{2 M_{ln} M_n}{\text{SNR}_{l,n}^{[b]}} \right)^{M_n} \text{U} \left(M_n, 1 + M_n - M_{ln}, \frac{2 M_{ln} M_n}{\text{SNR}_{l,n}^{[b]}} \right), \quad (27)$$

where M_n and M_{ln} are the Nakagami parameters for links TR and CT, respectively, while $\text{SNR}_{l,n}^{[b]}$ is the average received SNR for bistatic system. Under dyadic Rayleigh fading ($M_n = M_{ln} = 1$), **the diversity order is 1**.

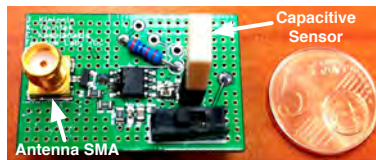
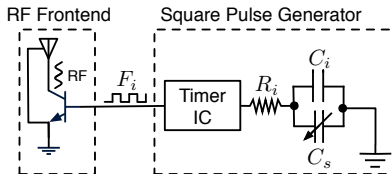
- The above BER bound coincides with noncoherent envelope bistatic scatter radio detection!

Some Numerical Results



- Wireless and signal parameters: Equal average received SNR, $M_n = 5.7619$ and $M_{ln} = 5.2632$.

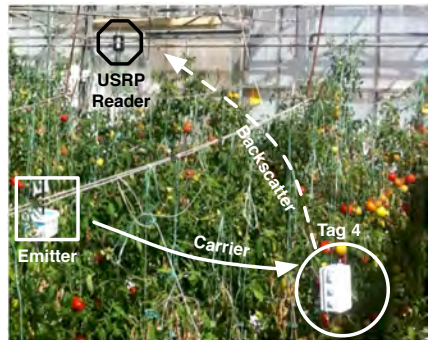
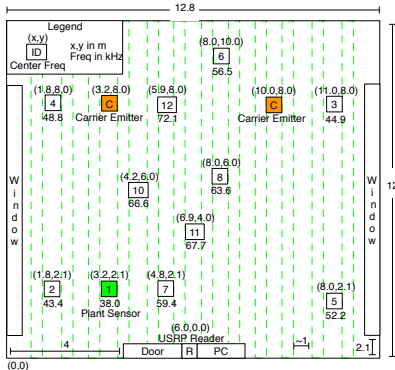
Greenhouse Environmental Humidity [22, 23]



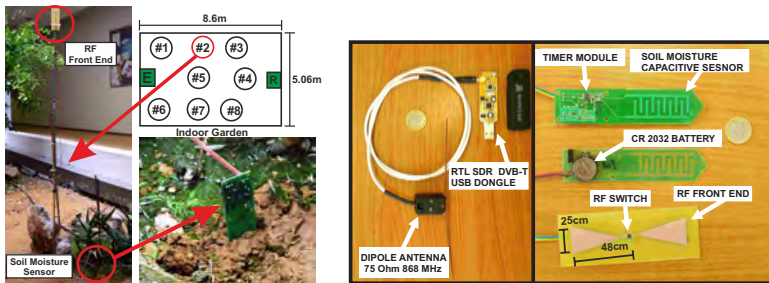
- Principle: capacitor changes \Rightarrow freq. of backscattered signal.
- Cost: \sim 3Euro (quantity of 1), Power: $220\mu\text{Watt}$, RMS: 1 – 2% RH.
- Networking: simple, multiple-access (FDMA).

[22] E. Kampionakis, J. Kimionis, K. Tountas, C. Konstantopoulos, E. Koutroulis, and A. Bletsas, "Wireless environmental sensor networking with analog scatter radio & timer principles", IEEE Sensors J., vol. 14, no. 10, pp. 3365-3376, Oct. 2014. **Conf. version [23] received IEEE Sensors Conf. 2013 distinction.**

Greenhouse Environmental Humidity [22, 23]



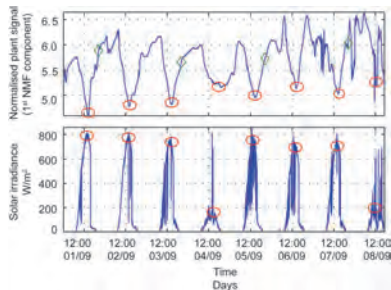
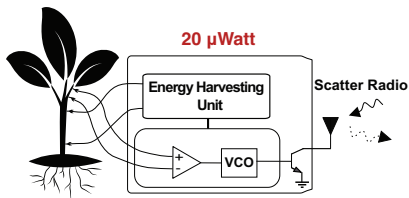
Soil Moisture Humidity Across a Field [24, 25]



- Principle: capacitor changes \Rightarrow freq. of backscattered signal.
- Cost: \sim 5Euro (quantity of 1), Power: $\sim 100\mu$ Watt, RMS: 1.9% RH.
- Networking: simple, multiple-access (FDMA).

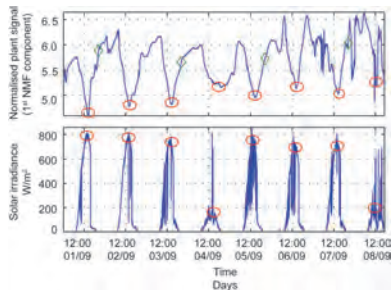
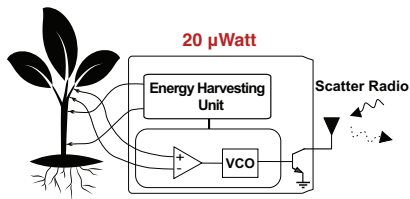
[24] S. N. Daskalakis, S. D. Assimonis, E. Kampianakis, and A. Bletsas, "Soil moisture scatter radio networking with low power", IEEE Trans. Microw. Theory Techn., vol. 64, no. 7, pp. 2338-2346, Jul. 2016.

Plants as Backscatter Sensors & Batteries [26],[27]



- Principle: measure Electric Potential (EP) across two electrodes in the plant stem.
- Transmit EP with backscatter FM. Use Plant as Battery.
- EP signal is correlated with solar irradiance and plant watering!

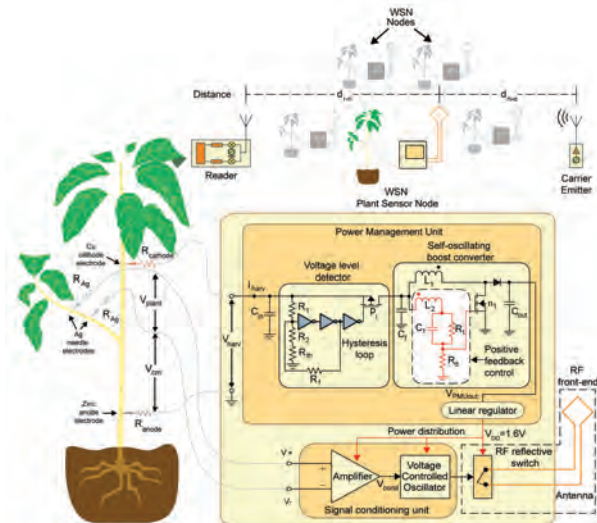
Plants as Backscatter Sensors & Batteries [26],[27]



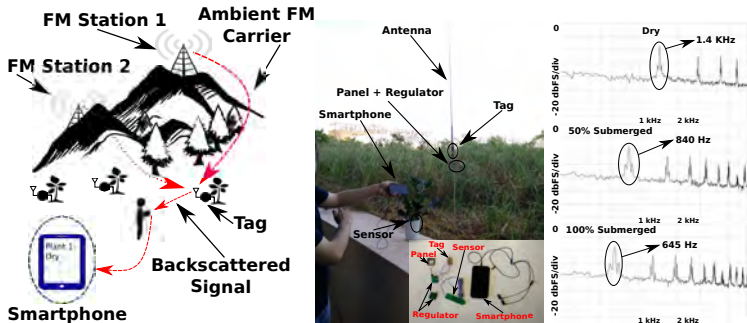
- Transmit EP with backscatter FM. Use Plant as Battery.
- EP signal is correlated with solar irradiance and plant watering!

[27] C. Konstantopoulos, E. Koutroulis, N. Mitianoudis, and A. Bletsas, "Converting a plant to a battery and wireless sensor with scatter radio and ultra-low cost", IEEE Trans. Instrum. Meas., vol. 65, no. 2, pp. 388-398, Feb. 2016. Conf. version at IEEE Sensors 2013 [26].

Plants as Backscatter Sensors & Batteries [26],[27]

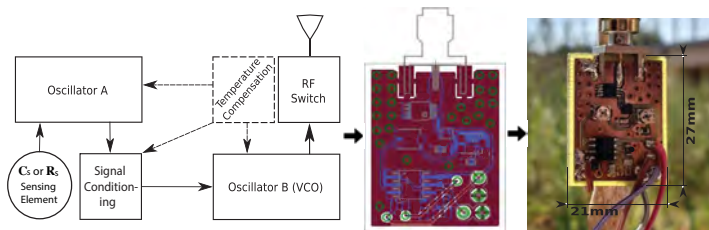


Ambient FM with μ Watt Sensors & Smartphone Transmit Diversity Reception [28]



- Principle: measure capacitance or resistance on top of Ambient FM.
- Receiver = Smartphone, emitter = Ambient FM.
- Exploit Transmit Diversity!

Ambient FM with μ Watt Sensors & Smartphone Transmit Diversity Reception [28]



- Sensor Power: 12 – 24 μ W (even in continuous, non-duty-cycled operation)!
- Tag-smartphone range: 26m, FM emitter-tag range: 6.5km!

[28] G. Vougioukas and A. Bletsas, "24 μ W 26m range batteryless backscatter sensors with FM remodulation and selection diversity", in Proc. IEEE RFID Techn. and Applications (RFID-TA), Warsaw, Poland, Sep. 2017.

Best Student Paper Award.

Questions Answered?

Questions for today:

- Maximum range/coverage?
...extended from tens-of-meters to kilometers under conditions...
- Connection to satellite/underwater communications?
...all require power-limited regime orthogonal signaling and symbol/sequence detection advances...
- “Can you measure the water soil moisture of your favorite flower using your cellphone”?
...yes, at μ Watt consumption (per tag sensor) cost...

Contributions

Ultra-low-power IoT technology:

- Ultra-low complexity, increased range, small processing delay, backscatter radio receivers.
- New, flexible, scatter radio network architectures with extended coverage.
- Noncoherent symbol-by-symbol and sequence detectors can be applied in specific ambient setups as well...

- [1] P. Alevizos, "Intelligent scatter radio, RF harvesting analysis, and resource allocation for ultra-low-power internet-of-things," Ph.D. dissertation, School of ECE, Technical University of Crete, Chania, Greece, 2017, advisor: A. Bletsas.
- [2] G. Vannucci, A. Bletsas, and D. Leigh, "A software-defined radio system for backscatter sensor networks," *IEEE Trans. Wireless Commun.*, vol. 7, no. 6, pp. 2170–2179, Jun. 2008.
- [3] J. D. Griffin and G. D. Durgin, "Gains for RF tags using multiple antennas," *IEEE Trans. Antennas Propag.*, vol. 56, no. 2, pp. 563–570, Feb. 2008.
- [4] J. Kimionis, A. Bletsas, and J. N. Sahalos, "Design and implementation of RFID systems with software defined radio," in *Proc. IEEE European Conf. on Antennas and Propagation (EuCAP)*, Prague, Czech Republic, Mar. 2012, pp. 3464–3468.
- [5] —, "Bistatic backscatter radio for tag read-range extension," in *Proc. IEEE RFID Techn. and Applications (RFID-TA)*, Nice, France, Nov. 2012.
- [6] —, "Bistatic backscatter radio for power-limited sensor networks," in *Proc. IEEE Global Commun. Conf. (GLOBECOM)*, Atlanta, GA, Dec. 2013, pp. 353–358.
- [7] —, "Increased range bistatic scatter radio," *IEEE Trans. Commun.*, vol. 62, no. 3, pp. 1091–1104, Mar. 2014.
- [8] V. Iyer, V. Talla, B. Kellogg, S. Gollakota, and J. Smith, "Inter-technology backscatter: Towards internet connectivity for implanted devices," in *Proceedings of the 2016 ACM SIGCOMM Conference*, ser. SIGCOMM '16. New York, NY, USA: ACM, 2016, pp. 356–369. [Online]. Available: <http://doi.acm.org/10.1145/2934872.2934894>
- [9] A. Bletsas, A. G. Dimitriou, and J. Sahalos, "Improving backscatter radio tag efficiency," *IEEE Trans. Microw. Theory Techn.*, vol. 58, no. 6, pp. 1502 – 1509, Jun. 2010.
- [10] V. Liu, A. Parks, V. Talla, S. Gollakota, D. Wetherall, and J. R. Smith, "Ambient backscatter: Wireless communication out of thin air," in *Proc. ACM SIGCOMM*, Hong Kong, China, 2013, pp. 39–50.
- [11] N. Fasarakis-Hilliard, P. N. Alevizos, and A. Bletsas, "Coherent detection and channel coding for bistatic scatter radio sensor networking," *IEEE Trans. Commun.*, vol. 63, pp. 1798–1810, May 2015.

- [12] P. N. Alevizos and A. Bletsas, "Noncoherent composite hypothesis testing receivers for extended range bistatic scatter radio WSNs," in *Proc. IEEE Int. Conf. on Commun.*, London, U.K., Jun. 2015.
- [13] P. N. Alevizos, A. Bletsas, and G. N. Karystinos, "Noncoherent short packet detection and decoding for scatter radio sensor networking," *IEEE Trans. Commun.*, vol. 65, no. 5, pp. 2128–2140, May 2017.
- [14] P. N. Alevizos, Y. Fountzoulas, G. N. Karystinos, and A. Bletsas, "Noncoherent sequence detection of orthogonally modulated signals in flat fading with log-linear complexity," in *Proc. IEEE Int. Conf. Acoustics, Speech, and Signal Processing (ICASSP)*, Brisbane, Australia, Apr. 2015, pp. 2974–2978.
- [15] —, "Log-linear-complexity GLRT-optimal noncoherent sequence detection for orthogonal and RFID-oriented modulations," *IEEE Trans. Commun.*, vol. 64, no. 4, pp. 1600–1612, Apr. 2016.
- [16] P. N. Alevizos, N. Fasarakis-Hilliard, K. Tountas, N. Agadacos, N. Kargas, and A. Bletsas, "Channel coding for increased range bistatic backscatter radio: Experimental results," in *Proc. IEEE RFID Techn. and Applications (RFID-TA)*, Tampere, Finland, Sep. 2014, pp. 38–43.
- [17] N. Kargas, F. Mavromatis, and A. Bletsas, "Fully-coherent reader with commodity SDR for Gen2 FM0 and computational RFID," *IEEE Wireless Commun. Lett.*, vol. 4, no. 6, pp. 617–620, Dec. 2015.
- [18] G. Vougioukas, S. N. Daskalakis, and A. Bletsas, "Could battery-less scatter radio tags achieve 270-meter range?" in *Proc. IEEE Wireless Power Transfer Conf. (WPTC)*, Aveiro, Portugal, May 2016, pp. 1–3.
- [19] J. F. Ensworth and M. S. Reynolds, "Every smart phone is a backscatter reader: Modulated backscatter compatibility with bluetooth 4.0 low energy (BLE) devices," in *Proc. IEEE RFID*, San Diego, CA, Apr. 2015, pp. 78–85.
- [20] V. Talla, M. Hesar, B. Kellogg, A. Najafi, J. R. Smith, and S. Gollakota, "Lora backscatter: Enabling the vision of ubiquitous connectivity," *Proc. ACM Interact. Mob. Wearable Ubiquitous Technol.*, vol. 1, no. 3, pp. 105:1–105:24, Sep. 2017.
- [21] P. N. Alevizos, K. Tountas, and A. Bletsas, "Multistatic scatter radio sensor networks for extended coverage," *IEEE Trans. Wireless Commun.*, 2018, accepted, to appear.

- [22] E. Kampianakis, J. Kimionis, K. Tountas, C. Konstantopoulos, E. Koutroulis, and A. Bletsas, "Wireless environmental sensor networking with analog scatter radio & timer principles," *IEEE Sensors J.*, vol. 14, no. 10, pp. 3365–3376, Oct. 2014.
- [23] —, "Backscatter sensor network for extended ranges and low cost with frequency modulators: Application on wireless humidity sensing," in *Proc. IEEE Sensors Conf. (Sensors)*, Baltimore, MD, USA, Nov. 2013.
- [24] S. N. Daskalakis, S. D. Assimonis, E. Kampianakis, and A. Bletsas, "Soil moisture scatter radio networking with low power," *IEEE Trans. Microw. Theory Techn.*, vol. 64, no. 7, pp. 2338–2346, Jul. 2016.
- [25] —, "Soil moisture wireless sensing with analog scatter radio, low power, ultra-low cost and extended communication ranges," in *Proc. IEEE Sensors Conf. (Sensors)*, Valencia, Spain, Nov. 2014, pp. 122–125.
- [26] C. Konstantopoulos, E. Kampianakis, E. Koutroulis, and A. Bletsas, "Wireless sensor node for backscattering electrical signals generated by plants," in *Proc. IEEE Sensors Conf. (Sensors)*, Baltimore, MD, USA, Nov. 2013.
- [27] C. Konstantopoulos, E. Koutroulis, N. Mitianoudis, and A. Bletsas, "Converting a plant to a battery and wireless sensor with scatter radio and ultra-low cost," *IEEE Trans. Instrum. Meas.*, vol. 65, no. 2, pp. 388–398, Feb. 2016.
- [28] G. Vougioukas and A. Bletsas, "24 μ W 26m range batteryless backscatter sensors with FM remodulation and selection diversity," in *Proc. IEEE RFID Techn. and Applications (RFID-TA)*, Warsaw, Poland, Sep. 2017.

THANK YOU! Questions?

Technical Univ. of Crete, located at Chania: come and visit us!

www.tuc.gr

www.ece.tuc.gr

<https://www.youtube.com/watch?v=uzdpFTBLNhU>

